AMERICAN SOCIETY FOR MICROBIOLOGY | Infection and Immunity

Mycobacterium tuberculosis Resists Stress by Regulating PE19 Expression

Pavithra Ramakrishnan,[a] Alisha M. Aagesen,[a] John D. McKinney,[c] Anna D. Tischler[a,b,c]

Department of Microbiology and Immunology[a] and Center for Infectious Diseases and Microbiology Translational Research,[b] University of Minnesota, Minneapolis, Minnesota, USA; Global Health Institute, Swiss Federal Institute of Technology, Lausanne (EPFL), Lausanne, Switzerland[c]

Mycobacterium tuberculosis **requires the phosphate-sensing signal transduction system Pst/SenX3-RegX3 to resist host immune responses. A Δ*pstA1* mutant lacking a Pst phosphate uptake system component is hypersensitive to diverse stress conditions *in vitro* and is attenuated *in vivo* due to constitutive expression of the phosphate starvation-responsive RegX3 regulon. Transcriptional profiling of the Δ*pstA1* mutant revealed aberrant expression of certain *pe* and *ppe* genes. PE and PPE proteins, defined by conserved N-terminal domains containing Pro-Glu (PE) or Pro-Pro-Glu (PPE) motifs, account for a substantial fraction of the *M. tuberculosis* genome coding capacity, but their functions are largely uncharacterized. Because some PE and PPE proteins localize to the cell wall, we hypothesized that overexpression of these proteins sensitizes *M. tuberculosis* to stress by altering cell wall integrity. To test this idea, we deleted *pe* and *ppe* genes that were overexpressed by Δ*pstA1* bacteria. Deletion of a single *pe* gene, *pe19*, suppressed hypersensitivity of the Δ*pstA1* mutant to both detergent and reactive oxygen species. Ethidium bromide uptake assays revealed increased envelope permeability of the Δ*pstA1* mutant that was dependent on PE19. The replication defect of the Δ*pstA1* mutant in NOS2$^{-/-}$ mice was partially reversed by deletion of *pe19*, suppressing that increased membrane permeability due to PE19 overexpression sensitizes *M. tuberculosis* to host immunity. Our data indicate that PE19, which comprises only a 99-amino-acid PE domain, has a unique role in the permeability of the *M. tuberculosis* envelope that is regulated to resist stresses encountered in the host.**

Over 15 years ago, the novel PE and PPE protein families were identified in the complete genome sequence of *Mycobacterium tuberculosis*; together, these proteins represent over 7% of the genome coding capacity (1). Despite the attention placed on these protein families, their functions remain largely uncharacterized. PE and PPE proteins are defined by conserved N-terminal domains of ~110 or ~180 amino acids that contain Pro-Glu (PE) or Pro-Pro-Glu (PPE) sequence motifs, respectively (1). Although PE and PPE proteins can be identified in the genomes of all sequenced members of the *Mycobacterium* genus, their expansion into large multiprotein families is restricted to the slow-growing pathogenic mycobacterial species, including *M. tuberculosis*, and associated with the expansion of the ESX type VII secretion systems (2). There is evidence that some PE and PPE proteins are exported to the bacterial cell surface or extracellular milieu in an ESX-dependent manner (3–6). ESX-dependent export requires specific sequences within the PE or PPE domain (7, 8), including a recently described YxxxD/E ESX secretion targeting motif located near the C terminus of the ~110-amino-acid PE domain (9).

The 99 PE proteins and 69 PPE proteins encoded by the *M. tuberculosis* H37Rv genome can be further divided into subfamilies based on C-terminal sequence motifs (2). The PE_PGRS (polymorphic GC-rich sequence) and PPE_MPTR (major polymorphic tandem repeat) subfamilies, which include 65 and 23 members, respectively, each have highly repetitive C-terminal sequences. The PPE-PPW (10 members) and PPE-SVP (24 members) subfamilies, in contrast, have C-terminal domains with well-conserved and nonrepetitive sequence motifs.

Given the variability of the PE and PPE C-terminal domains and their potential extracellular localization, some have speculated that PE or PPE protein antigen variation could enable the evasion of antigen-specific host immune responses (1). This theory has been fueled by observations that there is variation in certain *pe_pgrs* gene sequences among clinical isolates (10, 11) and that recombination leading to gene deletions can occur between different copies of the *pe* and *ppe* genes (12). There is, however, little evidence to support rapid alterations of *pe* and *ppe* gene sequences *in vivo* (13). In addition, a recent comparative analysis of *pe* and *ppe* sequences from 40 clinical isolates suggested the absence of evolutionary selective pressure on these genes, an observation incompatible with positive selective pressure from the immune response that drives antigenic variation (14). Finally, there is evidence from both human tuberculosis infection and animal models that the conserved PE and PPE domains are themselves antigenic, generating immune responses that can cross-react with other PE and PPE proteins of similar sequence (15–17).

Only a few PE or PPE proteins have been investigated either through the generation of *M. tuberculosis* genetic mutants or biochemical characterization of purified proteins. Genome-wide mutagenesis approaches indicate that most *pe* and *ppe* genes are not essential for *M. tuberculosis* replication either in laboratory culture or in an animal model (18–20), suggesting functional redundancy among members of the PE and PPE families. However, PE_P-

Received 21 July 2015 **Returned for modification** 17 August 2015
Accepted 16 December 2015

Accepted manuscript posted online 28 December 2015

Citation Ramakrishnan P, Aagesen AM, McKinney JD, Tischler AD. 2016. *Mycobacterium tuberculosis* resists stress by regulating PE19 expression. Infect Immun 84:735–746. doi:10.1128/IAI.00942-15.

Editor: S. Ehrt

Address correspondence to Anna D. Tischler, tischler@umn.edu.

Supplemental material for this article may be found at http://dx.doi.org/10.1128/IAI.00942-15.

GRS30 has been implicated in *M. tuberculosis* virulence (21), and several *pe* and *ppe* transposon insertion mutants have been identified in screens for genes involved in phagosome maturation arrest (22, 23). In addition, several PE proteins have enzymatic activity. LipY (PE_PGRS63) is a triacylglycerol lipase that is targeted to the cell wall in a manner dependent on the PE domain (8, 24, 25). PE_PGRS11 exhibits phosphoglycerate mutase activity *in vitro* (26). Finally, a conserved serine hydrolase fold has been identified in several PE and PPE proteins (27). One of these proteins, PE16, has *in vitro* esterase activity against short-chain fatty acid esters (28). These observations suggest that some PE and PPE proteins have specific enzyme activities that could be important for *M. tuberculosis* metabolism and physiology. However, since the majority of PE and PPE proteins do not have conserved domains suggestive of enzymatic activity, this is not likely to be a general property of all PE or PPE proteins.

Knowledge of the physiological growth conditions that induce the expression of specific PE and PPE proteins could help to elucidate their function. The *pe* and *ppe* genes are differentially regulated at the transcriptional level in response to a variety of environmental signals (29) and are frequently found among the differentially expressed genes in regulatory mutants (30, 31). In addition, there is evidence that some PE_PGRS family members are expressed specifically in granulomatous lesions (32). Therefore, the differential expression of PE and PPE proteins may be an adaptive response by *M. tuberculosis* to specific environmental conditions that promotes bacterial survival.

The *M. tuberculosis* phosphate starvation-responsive signal transduction system Pst/SenX3-RegX3 is a transcriptional regulatory system that is required for resistance to host immune defenses (33). The SenX3-RegX3 two-component system normally is activated by inorganic phosphate (P_i) starvation. The activation of the DNA binding response regulator RegX3 is inhibited when P_i is abundant through a poorly understood interaction with the Pst (phosphate-specific transport) P_i uptake system. A Δ*pstA1* mutant that lacks a membrane-spanning component of the Pst system exhibits constitutive activation of RegX3 and dysregulated expression of RegX3-dependent genes in P_i-rich medium. We previously demonstrated that the hypersensitivity of the Δ*pstA1* mutant to various stress conditions *in vitro* and to host immune responses *in vivo* was attributable to aberrant activation of RegX3, because these hypersensitivity phenotypes were suppressed by deletion of *regX3*.

Our results suggested that a RegX3-regulated factor(s) is responsible for both sensitivity to stress conditions *in vitro* and sensitivity to host immune responses *in vivo*. The pleiotropic phenotypes of the Δ*pstA1* mutant, particularly sensitivity to the cell wall-disrupting detergent sodium dodecyl sulfate (SDS), suggested a cell wall defect (33). As part of our previous studies, we performed transcriptional profiling to define the set of genes that are aberrantly expressed by Δ*pstA1* bacteria in a RegX3-dependent manner (33). Among this set of genes, there were several that encode PE and PPE proteins. Of the PE and PPE proteins that have been characterized to date, many are localized to the mycobacterial cell wall (3, 7, 8, 34–36). We hypothesized that the overexpression of cell wall-localized PE and/or PPE proteins in the Δ*pstA1* mutant sensitize these bacteria to stress by subtly altering the architecture or permeability of the cell wall. Here, we demonstrate that overexpression of the PE protein PE19 sensitizes the Δ*pstA1* mutant to cell wall and oxidative stress conditions *in vitro* by increasing cell envelope permeability. We further demonstrate that the overexpression of PE19 is partially responsible for attenuation of the Δ*pstA1* mutant in $NOS2^{-/-}$ mice. Our results suggest that the PE19 protein has a unique and important function in *M. tuberculosis* physiology and that its expression is carefully controlled to enable bacterial persistence.

MATERIALS AND METHODS

Bacterial strains and culture conditions. *M. tuberculosis* Erdman and derivative strains were grown at 37°C in Middlebrook 7H9 (Difco) liquid culture medium supplemented with 10% albumin-dextrose-saline (ADS), 0.5% glycerol, and 0.1% Tween 80 or on Middlebrook 7H10 (Difco) solid culture medium supplemented with 10% oleic acid-albumin-dextrose-catalase (OADC; BD Biosciences) and 0.5% glycerol. For cultivation of *M. tuberculosis* $mc^2$7000 (H37Rv ΔRD1, Δ*panCD*) (37) and derivative strains, complete Middlebrook 7H9 or 7H10 medium was supplemented with 50 μg/ml pantothenic acid (Sigma). Frozen stocks were prepared by growing liquid cultures to mid-exponential phase (OD_{600} of 0.6 to 0.8), adding glycerol to 15% final concentration, and storing aliquots at −80°C. For phosphate-limiting (P_i-free) 7H9 broth, a 100× liquid stock of 7H9 base was reconstituted without the addition of the P_i-buffering components (Na_2HPO_4, KH_2PO_4). 1× P_i-free 7H9 was made with 0.5% glycerol, 10% ADS, 0.1% Tween 80, and 50 mM morpholinepropanesulfonic acid (MOPS) buffer, pH 6.6. Doubling times were calculated from daily OD_{600} measurements taken over the first 72 h of growth after dilution of mid-exponential-phase (OD_{600} of 0.5) cultures to an OD_{600} of 0.05 in complete 7H9 medium.

Cloning of deletion and complementation constructs. Constructs for deletion of putative *pe-ppe* gene pairs or operons were generated in the allelic exchange vector pJG1100 (38), which contains the *aph* (kanamycin resistance), *hyg* (hygromycin resistance), and *sacB* (sucrose sensitivity) markers (see Table S1 in the supplemental material). Genomic regions of ~800 bp 5′ and 3′ of the genes to be deleted were PCR amplified from *M. tuberculosis* Erdman genomic DNA using the oligonucleotides listed in Table S2. Reverse primers to amplify the 5′ regions were designed with an AvrII restriction site in-frame with the translation start codon. Forward primers to amplify the 3′ regions were designed with an AvrII restriction site in-frame with the stop codon. Resulting PCR products were cloned in pCR2.1-TOPO (Invitrogen) and sequenced. The 5′ and 3′ regions were removed from pCR2.1 by restriction with PacI/AvrII or AvrII/AscI, respectively, and ligated together in pJG1100 between the PacI and AscI sites to generate in-frame deletion constructs. Deletion constructs generated in pJG1100 and the genes they are designed to delete are listed in Table S1.

For complementation of the Δ*ppe27-pe19* and Δ*pe19* deletions, the *ppe27-pe19* locus or the full-length *pe19* gene was PCR amplified from *M. tuberculosis* Erdman genomic DNA using the primers indicated in Table S2 in the supplemental material. For the complementation of the Δ*pe19* deletion with C-terminal His_6 or hemagglutinin (HA) epitope-tagged versions of PE19, the full-length *pe19* gene was PCR amplified from *M. tuberculosis* Erdman genomic DNA using primer 1791compF and the reverse primers indicated in Table S2. The resulting PCR products were cloned in pCR2.1-TOPO and sequenced. For *ppe27-pe19* complementation, the insert was removed from pCR2.1 by digestion with ClaI and HpaI and cloned in similarly digested pMV261 to generate pMV*ppe27-pe19*. For *pe19* complementation, the inserts were removed from pCR2.1 by digestion with PstI and HindIII and cloned in similarly digested pMV261 to generate pMV*pe19*, pMV*pe19His6*, or pMV*pe19HA*.

***M. tuberculosis* strain construction.** *M. tuberculosis* strains harboring in-frame unmarked deletions were generated by a two-step homologous recombination allelic exchange method (39, 40). Deletions constructed and the vectors used to generate them are listed in Table S1 in the supplemental material. Plasmids were introduced into wild-type (WT) or Δ*pstA1* mutant (33) *M. tuberculosis* Erdman by electroporation with 1 to 2 μg of purified plasmid DNA. Electrocompetent *M. tuberculosis* strains were prepared as previously described (33). Transformants were grown

for 24 h in 7H9 broth before selecting recombinants containing chromosomally integrated pJG1100 on 7H10 agar containing kanamycin (15 μg/ml) and hygromycin (50 μg/ml). Kan^r/Hyg^r colonies were picked and grown in 7H9 broth without antibiotics to mid-exponential phase. Integration of the constructs at the correct chromosomal locus was confirmed by PCR on heat-inactivated cell lysates using the primer pairs for detection of the 5′ and 3′ integrations (see Table S3). Clones that contained the allelic exchange vector integrated at the correct locus were serially diluted and plated on 7H10 agar containing 2% sucrose for counterselection of the pJG1100 vector. Sucrose-resistant clones were grown in 7H9 broth, and isolates in which the deletion replaced the wild-type allele were identified by PCR using the primers for detection of the gene deletion (see Table S3). The Δ*pstA1* mutation was constructed in *M. tuberculosis* $mc^2$7000 as described previously (33). The Δ*pe19* deletion was constructed in $mc^2$7000 WT and Δ*pstA1* backgrounds as described above. Analysis of phthiocerol dimycocerosate (PDIM) production was done by thin-layer chromatography of [^{14}C]propionate-labeled lipid extracts as previously described (38).

For complementation of the Δ*pe19* mutation, the Δ*pe19* and Δ*pstA1* Δ*pe19* strains were made electrocompetent as described above and electroporated with plasmid pMV*pe19*. Transformants were selected on 7H10 agar containing kanamycin (15 μg/ml). The presence of the complementing plasmid in Kan^r isolates was confirmed by PCR on heat-inactivated cell lysates using primers pMVinsF/1791compR.

Southern hybridization. Genomic DNA was extracted from WT *M. tuberculosis* Erdman, the Δ*pstA1* mutant, and the indicated *pe-ppe* deletion mutants as described previously (41). Equivalent amounts of genomic DNA were digested overnight with the restriction enzymes BamHI, KpnI, or SalI. Restricted DNA was separated by electrophoresis on a Tris-acetate-EDTA (TAE) agarose gel and transferred to a Hybond N+ nylon membrane (Amersham). Probes were generated by PCR amplification from *M. tuberculosis* Erdman genomic DNA using primers 1787F/1787R, 3622F/3622R, or 1790F/1790R (see Table S2 in the supplemental material) and labeled using the ECL direct nucleic acid labeling kit (Amersham) according to the manufacturer's instructions. The blot was blocked with Amersham Gold hybridization buffer prepared with 250 mM NaCl and 5% (wt/vol) blocking reagent for 2.5 h at 42°C. The labeled probe was added and the blot was incubated overnight at 42°C. The membrane was washed according to the manufacturer's instructions, and the probe was detected with ECL detection reagents (Amersham). Autoradiographic films (Kodak) were exposed to the blots for 1 to 5 min and developed on an automatic film processor.

qRT-PCR. For confirmation of the transcriptional profiling results, bacteria were grown to mid-exponential phase (OD_{600} of 0.5) in 7H9 broth. To assess the response to P_i starvation, bacteria were grown to mid-exponential phase in 7H9 broth and then washed twice and resuspended to an OD_{600} of 0.05 in P_i-free 7H9 broth. Cultures were incubated at 37°C, and bacteria were collected for RNA extraction at 0, 24, 48, 72, and 96 h. Cells were collected by centrifugation (4,700 × *g*, 10 min, 4°C), and RNA was extracted as described previously (33). Equivalent amounts of total RNA were treated with Turbo DNase (Ambion) and reverse transcribed to cDNA with the Transcriptor first-strand cDNA synthesis kit (Roche) using random hexamers for priming and the following cycling conditions: 10 min annealing at 25°C, 60 min extension at 50°C, and 5 min heat inactivation at 85°C. cDNA was stored at −20°C until real-time PCRs were performed. Quantitative real-time reverse transcription-PCRs (qRT-PCRs) were prepared with 2× LightCycler 480 Sybr green I master mix (Roche), 2 μl cDNA, and 0.3 μM primers and were run in absolute quantification mode on a LightCycler 480 (Roche). PCR cycling conditions were 95°C for 10 min; 45 cycles of 95°C for 10 s, 60°C for 20 s, and 72°C for 20 s with data collected once per cycle during the extension phase; and one cycle of 95°C for 5 s, 60°C for 1 min, and 97°C with a ramp rate of 0.11°C/s to generate melting curves for confirmation of product specificity. Mock reactions (no RT) were performed on each sample to confirm the absence of genomic DNA contamination. Cp values were converted to copy numbers using standard curves for each gene. Target cDNA was internally normalized to *sigA* cDNA (P_i-rich cultures) or 16S cDNA (P_i-starved cultures). Primers for qRT-PCR used in this study are listed in Table S2 in the supplemental material. Primers were designed using Primer Express software (Applied Biosystems) and were tested in standard PCRs using 100 *M. tuberculosis* genome equivalents as the template.

Cell wall and ROS stress. Bacteria were grown to mid-exponential phase (OD_{600} of 0.5) in 7H9 broth, diluted to an OD_{600} of 0.05 in fresh 7H9 broth, and incubated at 37°C after addition of 0.125% SDS or 3 mM hydrogen peroxide (H_2O_2). CFU were enumerated at 0 and 24 h by plating serially diluted culture aliquots on 7H10 agar.

Reactive nitrogen species (RNS) stress. Bacteria were grown to mid-exponential phase (OD_{600} of 0.5) in 7H9 broth and treated with the NO donor diethylenetriamine-NONOate (DETA-NO; Sigma) as described previously (42), except that complete 7H9 broth was used. DETA-NO was added at 0, 24, and 48 h. CFU were enumerated at 0 and 72 h by plating serially diluted culture aliquots on 7H10 agar.

Acidic pH stress. Bacteria were grown to mid-exponential phase (OD_{600} of 0.5) in 7H9 broth, diluted to an OD_{600} of 0.05 in fresh 7H9 broth at pH 5.5, and incubated at 37°C. CFU were enumerated at 0, 2, 4, and 7 days by plating serially diluted culture aliquots on 7H10 agar.

Ethidium bromide uptake. The accumulation of ethidium bromide was measured as previously described (43). *M. tuberculosis* $mc^2$7000 and derivative strains were grown to mid-exponential phase (OD_{600} of 0.6 to 1.0), pelleted by centrifugation at room temperature, and resuspended in ethidium bromide uptake buffer (50 mM KH_2PO_4 [pH 7.0], 5 mM $MgSO_4$) to an OD_{600} of 0.5. Cells were preenergized with 25 mM glucose (Sigma) for 5 min. Ethidium bromide was added at a final concentration of 20 μM. Uptake was measured at room temperature using black, flat-bottom 96-well microplates (Corning Costar) and a SpectraMax M5 microplate reader (Molecular Devices, LLC) in top-reading mode with excitation at 530 nm and emission at 590 nm.

Mouse infections. Male and female $NOS2^{-/-}$ and C57BL/6J mice 6 to 8 weeks of age were purchased from Jackson Laboratory. $Irgm1^{-/-}$ mice (44) were bred under specific-pathogen-free conditions at the EPFL Center of Phenogenomics or the University of Minnesota Research Animal Resources. All mouse strains were on the C57BL/6 background. Mice were infected via the aerosol route with ~100 CFU using either a custom-built aerosol chamber as described previously (38) or an inhalation exposure system (GlasCol). For experiments using the inhalation exposure system, the nebulizer was loaded with a bacterial suspension in PBS containing 0.05% Tween 80 at an OD_{600} of 0.01, and mice were exposed to the aerosol for 20 min. Infected mice were euthanized by CO_2 overdose. Bacterial CFU were enumerated by plating serially diluted lung homogenates on 7H10 agar and counting colonies after 3 to 4 weeks of incubation at 37°C. The animal protocols used in this study were reviewed and approved by the chief veterinarian of EPFL, the Service de la Consommation et des Affaires Vétérinaires of the Canton of Vaud, the Swiss Office Vétérinaire Fédéral, and the University of Minnesota Institutional Animal Care and Use Committee. All animal experiments were done in strict accordance with the recommendations in the *Guide for the Care and Use of Laboratory Animals* of the National Institutes of Health (45) and the Swiss Law for the Protection of Animals.

Statistical analysis. Student's unpaired *t* test (two-tailed) was used for pairwise comparisons between WT and mutant strains of *M. tuberculosis*. The Mantel-Cox log-rank test was used for comparison of Kaplan-Meier plots of mouse survival. *P* values were calculated using GraphPad Prism 5.0 software (GraphPad Software, Inc.). $P < 0.05$ was considered significant.

RESULTS

PstA1 negatively regulates expression of specific *pe* and *ppe* genes. Using transcriptional profiling, we previously identified a subset of *pe* and *ppe* genes that were differentially expressed by Δ*pstA1* bacteria relative to a wild-type (WT) control during

TABLE 1 *pe* and *ppe* genes differentially expressed by *M. tuberculosis* Δ*pstA1* mutant[a]

Gene	Rv numbering	Differential gene expression			
		Δ*pstA1* vs WT		Δ*pstA1* Δ*regX3* vs WT	
		Ratio	*P* value	Ratio	*P* value
ppe65	*rv3621*	12.245	0.00438	1.004	0.987
pe32	*rv3622*	11.616	0.00362	0.847	0.405
ppe25	*rv1787*	9.775	0.000088	1.775	0.243
ppe27	*rv1790*	6.819	0.000234	1.284	0.652
pe18	*rv1788*	3.625	0.000952	1.006	0.99
pe19[b]	*rv1791*	4.089	0.0645	1.260	0.706
ppe19	*rv1361*	3.176	0.0207	0.752	0.251
pe15	*rv1386*	0.0846	0.00111	1.364	0.705
ppe20	*rv1387*	0.0797	0.0273	2.022	0.15
pe31	*rv3477*	0.0237	0.00009	1.676	0.217

[a] Expression ratios were determined by microarray analysis using RNA extracted from bacteria grown in P_i-rich 7H9 medium. Data are reproduced from reference 33.
[b] Did not achieve *P* value cutoff of <0.05.

growth in P_i-rich medium (Table 1; data are reproduced from reference 33). Each of the differentially expressed *pe* genes encodes only a PE domain. Each of the overexpressed *ppe* genes encodes a protein from the PPE-SVP subfamily, while the underexpressed *ppe20* gene (*rv1387*) encodes a PPE-PPW subfamily protein (2). Transcript abundance for each of these genes was restored to the wild-type level by deletion of *regX3* (Table 1) (33). These data suggested that some *pe* and *ppe* genes are regulated by the Pst/SenX3-RegX3 signal transduction system, and that PstA1 is required to negatively regulate their expression when P_i is readily available. To confirm the transcriptional profiling data, we examined transcript levels of several differentially expressed *pe* and *ppe* genes by quantitative real-time RT-PCR (qRT-PCR) in RNA extracted from bacteria grown in P_i-rich medium. Consistent with the transcriptional profiling data, we found that the *ppe25*, *pe19*, and *ppe65* genes were significantly overexpressed by Δ*pstA1* mutant bacteria in a RegX3-dependent manner (Fig. 1A). The fold increase in expression ranged from 4-fold for *pe19* to 35-fold for *ppe65*. The aberrant gene expression pattern characteristic of the Δ*pstA1* mutant was restored by complementation of the Δ*regX3* deletion in *trans* (Fig. 1A). These data suggest that the expression of certain *pe* and *ppe* genes is controlled by the Pst/SenX3-RegX3 system.

We previously demonstrated that transcription of *ppe20* is repressed in a RegX3-dependent manner during P_i limitation and is constitutively repressed in the Δ*pstA1* mutant (33). In contrast, we predicted that *pe19* expression would be induced by P_i limitation in a RegX3-dependent manner. The abundance of the *pe19* transcript was increased 6-fold in WT *M. tuberculosis* within 24 h of P_i limitation. This induction of *pe19* transcription was statistically significant and required RegX3 (Fig. 1B). These data confirm that some *pe* and *ppe* genes are regulated by the Pst/SenX3-RegX3 system in response to available P_i.

Deletion of the *ppe27-pe19* locus suppresses sensitivity to cell wall and reactive oxygen stress. We previously showed that Δ*pstA1* bacteria are hypersensitive to a variety of stress conditions *in vitro*, and that this stress sensitivity can be attributed to aberrant RegX3-dependent transcription (33). To test if overexpression of specific *pe* and/or *ppe* genes is responsible for stress hypersensitivity of the Δ*pstA1* mutant, we constructed four deletions of gene pairs or putative operons encoding PE and PPE proteins that were highly overexpressed by Δ*pstA1* bacteria (Δ*ppe25-pe19*, Δ*ppe25-ppe26*, Δ*ppe27-pe19*, and Δ*pe32-ppe65*) (Fig. 2D and E). In-frame, unmarked deletions were constructed by two-step homologous recombination in both the WT and Δ*pstA1* mutant strain backgrounds and were confirmed by PCR (data not shown) and Southern blotting (Fig. 2A and C). Notably, several of the deletions caused a growth defect in standard P_i-rich 7H9 medium. The Δ*ppe25-pe19* and Δ*ppe27-pe19* deletion mutations caused a significant increase in the doubling time, independent of the strain background in which the deletions were constructed (Table 2). The Δ*ppe25-pe19* and Δ*ppe27-pe19* mutants also formed smaller colonies on 7H10 solid agar medium independent of the strain background (data not shown). The growth defect of the Δ*ppe27-pe19* mutants was only partially complemented by providing the *ppe27-pe19* locus in *trans* (Table 2), suggesting polarity of the Δ*ppe27-pe19* deletion on downstream gene expression. Nevertheless, these data indicate that the *ppe27-pe19* locus plays an important role in *M. tuberculosis* physiology to enable optimal replication *in vitro*.

Because Δ*pstA1* bacteria exhibit hypersensitivity to either the cell wall-disrupting detergent SDS or the reactive oxygen species

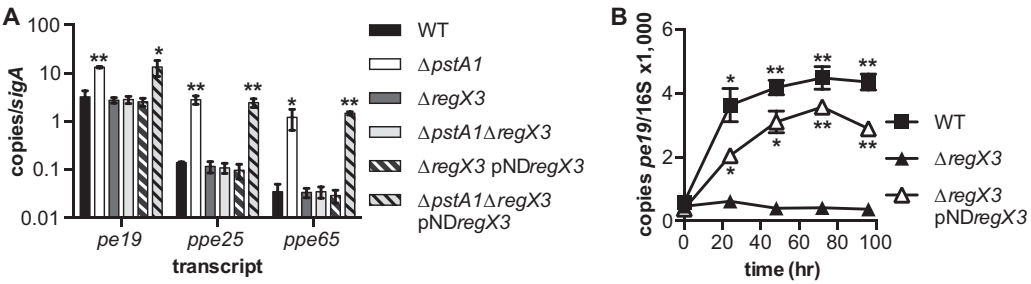

FIG 1 Specific *pe* and *ppe* genes are regulated by Pst/SenX3-RegX3. (A) RNA was extracted from cultures of *M. tuberculosis* WT, Δ*pstA1*, Δ*regX3*, Δ*pstA1*Δ*regX3*, Δ*regX3* pND*regX3*, and Δ*pstA1*Δ*regX3* pND*regX3* strains grown to mid-exponential phase (OD_{600} of 0.5) in P_i-rich 7H9 medium. The abundance of *ppe25*, *pe19*, and *ppe65* transcripts relative to that of *sigA* was determined by real-time quantitative RT-PCR. Data shown are the means ± standard deviations from three independent experiments. Asterisks indicate statistically significant differences from the WT: *, $P < 0.05$; **, $P < 0.001$. (B) RNA was extracted from cultures of *M. tuberculosis* WT, Δ*regX3*, and Δ*regX3* pND*regX3* strains at the indicated times after shifting to P_i-free 7H9 medium. *pe19* transcript abundance relative to that of 16S rRNA was determined by real-time quantitative RT-PCR. Data shown are the means ± standard deviations from three independent experiments. Asterisks indicate statistically significant differences from both the respective 0-h time point and the Δ*regX3* mutant: *, $P < 0.005$; **, $P < 0.0005$.

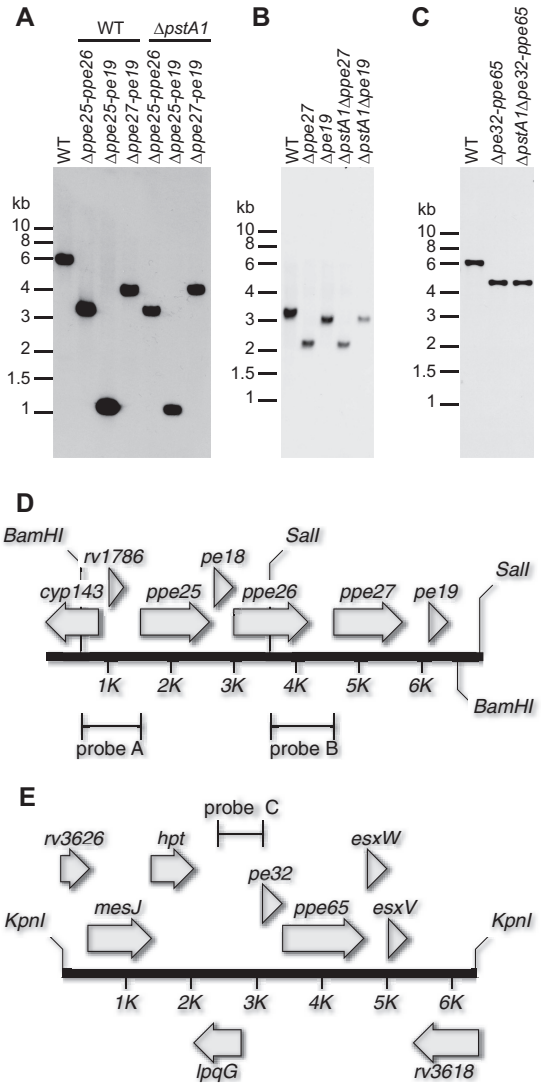

FIG 2 Southern blotting confirms *pe-ppe* deletions. (A to C) Southern blots. Genomic DNA from *pe-ppe* deletion strains and the *M. tuberculosis* wild type (WT) was digested with the indicated restriction enzymes. Bands that hybridized to a gene-specific probe were detected by enhanced chemiluminescence. Positions of molecular size markers are indicated. The *pe-ppe* deletions are expected to remove the following lengths of DNA sequence: Δ*ppe25-pe19*, 4.89 kbp; Δ*ppe25-ppe26*, 2.66 kbp; Δ*ppe27-pe19*, 1.80 kbp; Δ*ppe27*, 1.10 kbp; Δ*pe19*, 0.30 kbp; Δ*pe32-ppe65*, 2.65 kbp. (A) BamHI digest, probe A (primers 1787F/1787R); (B) SalI digest, probe B (primers 1790F/1790R); (C) KpnI digest, probe C (primers 3622F/3622R). (D and E) Maps of the mutated *pe-ppe* loci. Genes are indicated by gray arrows. Lines indicate locations of BamHI, SalI, and KpnI restriction enzyme sites and probes used for Southern blotting. (D) *ppe25-pe19* locus. (E) *pe32-ppe65* locus.

H_2O_2, we first tested if any of the *pe-ppe* deletions altered resistance to these two stress conditions. Deletion of either *pe32-ppe65* or *ppe25-ppe26* in the Δ*pstA1* mutant had no significant effect on sensitivity to SDS or H_2O_2 (Fig. 3A). In contrast, the Δ*ppe25-pe19* and Δ*ppe27-pe19* deletions both reversed the hypersensitivity of the Δ*pstA1* mutant to SDS and H_2O_2. The Δ*pstA1*Δ*ppe25-pe19* and Δ*pstA1*Δ*ppe27-pe19* mutants exhibited no significant difference in resistance to either SDS or H_2O_2 compared to the WT control (Fig. 3A). The Δ*ppe25-pe19* and Δ*ppe27-pe19* deletions also significantly increased SDS resistance in the WT strain background, suggesting that basal expression of the *ppe27-pe19* locus contributes to sensitivity to cell wall stress (Fig. 3A).

Overexpression of *pe19* sensitizes *M. tuberculosis* to cell wall and oxidative stress. To further elucidate which genes are involved in sensitivity to cell wall or oxidative stress, we constructed independent in-frame unmarked deletions of the *ppe27* and *pe19* genes in both WT Erdman and the Δ*pstA1* mutant. The Δ*ppe27* and Δ*pe19* deletions were confirmed by PCR (data not shown) and Southern blotting (Fig. 2B). The Δ*ppe27* mutation had no impact on the growth rate in either the WT or Δ*pstA1* mutant backgrounds (Table 2). In contrast, the Δ*pe19* and Δ*pstA1* Δ*pe19* mutants both had significantly reduced growth rates in standard P_i-rich 7H9 medium (Table 2 and Fig. 4). Both strains harboring the Δ*pe19* deletion also formed smaller colonies than the parental strain on 7H10 agar medium (data not shown). These growth phenotypes were fully complemented by providing a copy of the *pe19* gene on the episomal plasmid pMV261 under the control of the strong constitutive *hsp60* promoter (Table 2 and Fig. 4).

The Δ*ppe27* and Δ*pe19* strains were tested for resistance to both SDS and H_2O_2. The Δ*ppe27* mutation did not alter sensitivity to either stress condition (Fig. 3B). In contrast, the Δ*pe19* mutation fully suppressed sensitivity of the Δ*pstA1* mutant to both SDS and H_2O_2 (Fig. 3B). Complementation of the Δ*pe19* mutation with the pMV*pe19* plasmid restored the hypersensitivity to SDS and H_2O_2 characteristic of Δ*pstA1* bacteria, confirming that *pe19* is responsible for these stress sensitivity phenotypes (Fig. 3C). These data suggest that overexpression of *pe19* causes sensitivity of the Δ*pstA1* mutant to SDS and H_2O_2 stress. The pMV*pe19* plasmid also caused increased sensitivity to SDS and H_2O_2 in both the WT and Δ*pe19* strain backgrounds, although the change in H_2O_2 sensitivity did not achieve statistical significance (Fig. 3C). To test if *pe19* is overexpressed from the pMV*pe19* plasmid, we examined the level of *pe19* transcript by qRT-PCR in strains harboring the complementation plasmid. Although the difference was not statistically significant, the *pe19* gene was expressed at a 2.5-fold higher level in the Δ*pe19* pMV*pe19* strain than in the WT control (Fig. 5A). These data suggest that increased expression of *pe19* is sufficient to cause hypersensitivity to cell wall and oxidative stress.

TABLE 2 Doubling times of *pe-ppe* deletion mutants in P_i-rich 7H9 medium[a]

pe-ppe deletion	Doubling time[b] (h), WT background	*P* value (vs WT)	Doubling time[b] (h), Δ*pstA1* background	*P* value (vs Δ*pstA1*)
None	19.41 ± 1.59		19.71 ± 1.70	
Δ*pe32-ppe65*	20.99 ± 0.50	0.1314	18.92 ± 0.92	0.4704
Δ*ppe25-pe19*	27.63 ± 4.29	0.0004	27.73 ± 2.19	<0.0001
Δ*ppe25-ppe26*	20.87 ± 0.34	0.1568	19.50 ± 0.88	0.8509
Δ*ppe27-pe19*	28.32 ± 2.55	<0.0001	25.86 ± 2.19	0.0005
Δ*ppe27-pe19* pMV*ppe27-pe19*	23.25 ± 0.98	0.0236	21.77 ± 1.13	0.1554
Δ*ppe27*	18.54 ± 0.24	0.4018	18.15 ± 0.33	0.1937
Δ*pe19*	22.67 ± 0.87	0.003	22.95 ± 2.52	0.0137
Δ*pe19* pMV-*pe19*	20.70 ± 0.93	0.2210	19.65 ± 0.61	0.9581

[a] Doubling times were determined from optical density measurements taken during the first 72 h of growth after dilution to an OD_{600} of 0.05 in 7H9 medium.
[b] Means ± standard deviations of doubling times from three independent cultures.

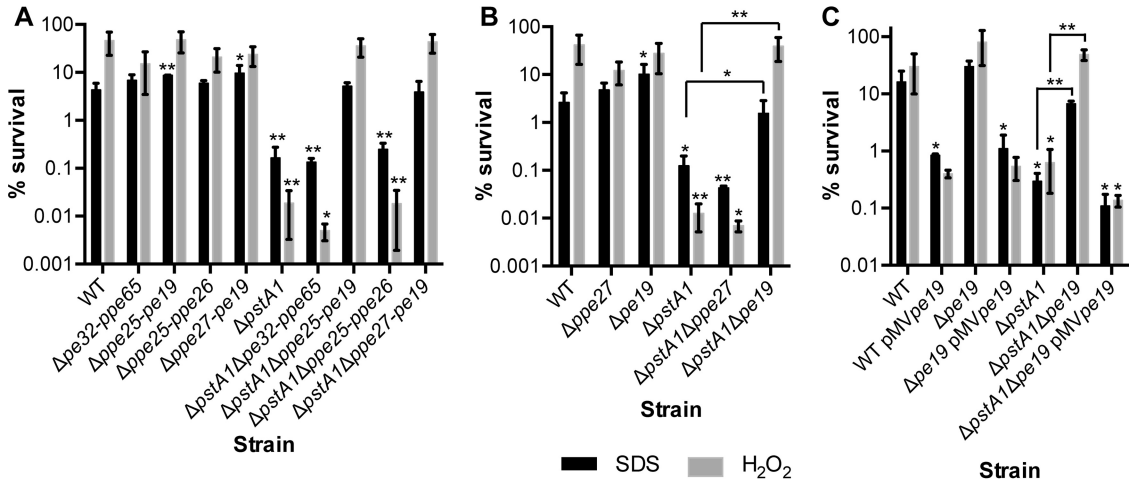

FIG 3 Hypersensitivity of the Δ*pstA1* mutant to cell wall and reactive oxygen stress is suppressed by deletion of *pe19*. The indicated *M. tuberculosis* strains were grown to mid-exponential phase (OD_{600} of 0.5) in 7H9 medium and diluted to an OD_{600} of 0.05 in fresh 7H9 medium. Sodium dodecyl sulfate (SDS) or hydrogen peroxide (H_2O_2) was added at 0.125% or 3 mM final concentration, respectively, and cultures were incubated at 37°C with shaking. CFU were enumerated at 0 and 24 h by plating serially diluted cultures on 7H10 agar medium and incubating at 37°C for 3 to 4 weeks. Percent survival was calculated as (CFU poststress)/(CFU prestress) × 100. Results presented are the means ± standard deviations from at least three independent experiments. (A) Deletions of putative *pe-ppe* operons Δ*pe32-ppe65*, Δ*ppe25-pe19*, Δ*ppe25-ppe26*, and Δ*ppe27-pe19* in the WT and Δ*pstA1* parental strain backgrounds. (B) Individual Δ*ppe27* and Δ*pe19* mutations in the WT and Δ*pstA1* parental strain backgrounds. (C) Complementation of the Δ*pe19* deletion. Asterisks indicate statistically significant differences from the WT control: *, $P < 0.05$; **, $P < 0.005$.

Although the data suggest that PE19 directly mediates changes in stress sensitivity, an alternative possibility is that PE19 normally participates in the Pst/SenX3-RegX3 signal transduction pathway. In this scenario, deletion of *pe19* would cause global changes in the expression of genes that are controlled by the Pst/SenX3-RegX3 system. We tested the expression of several genes that we previously showed were overexpressed by Δ*pstA1* bacteria in a RegX3-dependent manner (33). Deletion of *pe19* did not alter transcription of any of these known targets of Pst/SenX3-RegX3 regulation (Fig. 5B). There were no significant differences in transcript levels between the WT and Δ*pe19* strains or between the Δ*pstA1* and Δ*pstA1* Δ*pe19* strains. These data suggest that PE19 is not involved

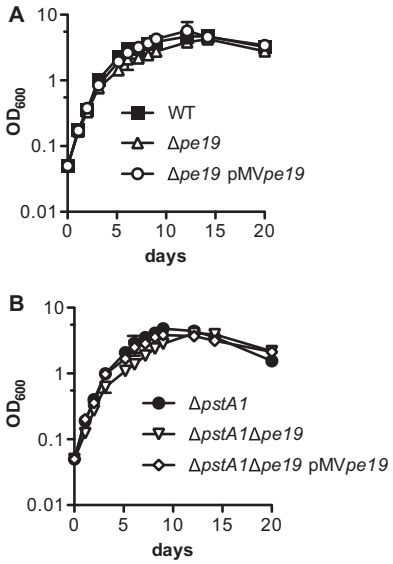

FIG 4 *pe19* deletion mutants have a growth defect in liquid culture. *M. tuberculosis* WT, Δ*pe19*, Δ*pe19* pMV*pe19*, Δ*pstA1*, Δ*pstA1* Δ*pe19*, and Δ*pstA1* Δ*pe19* pMV*pe19* strains were grown to mid-exponential phase (OD_{600} of 0.5) in 7H9 medium, diluted to an OD_{600} of 0.05 in fresh 7H9 medium, and incubated with shaking at 37°C. Aliquots of each culture were taken at the indicated times for measurement of the OD_{600}. Results are averages ± standard deviations from triplicate cultures and are representative of two independent experiments.

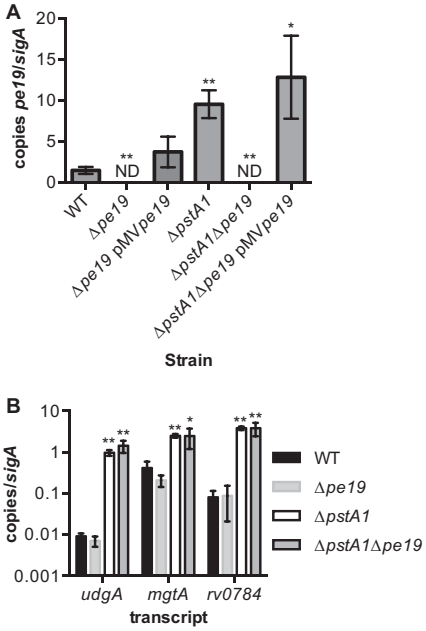

FIG 5 Gene expression in *pe19* deletion mutant and complemented strains. RNA was extracted from cultures of *M. tuberculosis* WT, Δ*pe19*, Δ*pe19* pMV*pe19*, Δ*pstA1*, Δ*pstA1* Δ*pe19*, and Δ*pstA1* Δ*pe19* pMV*pe19* strains grown to mid-exponential phase (OD_{600} of 0.5) in P_i-rich 7H9 medium. The abundance of *pe19* (A) and *udgA*, *mgtA*, and *rv0784* (B) transcripts relative to that of *sigA* was determined by real-time quantitative RT-PCR. Data shown are the means ± standard deviations from three independent experiments. ND indicates no detectable transcript. Asterisks indicate statistically significant differences from the WT: *, $P < 0.01$; **, $P < 0.005$.

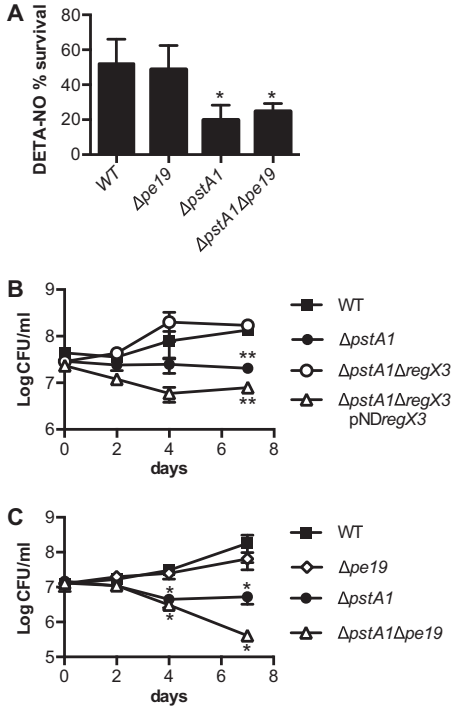

FIG 6 *pe19* deletion does not suppress sensitivity of the Δ*pstA1* mutant to reactive nitrogen or acidic pH stress. The indicated *M. tuberculosis* strains were grown to mid-exponential phase (OD_{600} of 0.5) in 7H9 medium before being subjected to reactive nitrogen or acidic pH stress conditions. CFU were enumerated by plating serially diluted cultures on 7H10 agar medium and incubating at 37°C for 3 to 4 weeks. Results presented are the averages ± standard deviations from triplicate cultures and are representative of two independent experiments. (A) Reactive nitrogen stress. Cultures were diluted to an OD_{600} of 0.05 in 7H9 medium and incubated at 37°C with shaking. DETA-NO was added to cultures at 0.2 mM final concentration at 0, 24, and 48 h. CFU were enumerated at 0 and 72 h. Percent survival was calculated at (CFU poststress)/(CFU prestress) × 100. (B and C) The indicated strains were diluted to an OD_{600} of 0.05 in 7H9 medium acidified to pH 5.5. CFU were enumerated at 0, 2, 4, and 7 days. Asterisks indicate statistically significant differences from the WT control: *, $P < 0.05$; **, $P < 0.0005$.

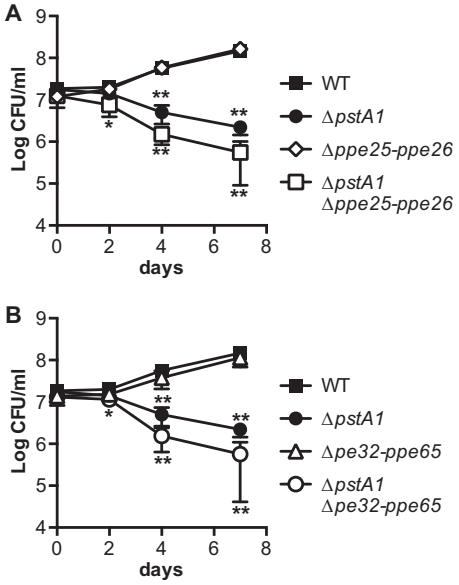

FIG 7 Δ*ppe25-ppe26* and Δ*pe32-ppe65* deletions do not suppress sensitivity of the Δ*pstA1* mutant to acidic pH stress. The indicated *M. tuberculosis* strains were grown to mid-exponential phase (OD_{600} of 0.5) in 7H9 medium, diluted to an OD_{600} of 0.05 in 7H9 medium acidified to pH 5.5, and incubated at 37°C with shaking. CFU were enumerated at 0, 2, 4, and 7 days by plating serially diluted cultures on 7H10 agar medium and incubating at 37°C for 3 to 4 weeks. Results presented are the averages ± standard deviations from three independent experiments. Asterisks indicate statistically significant differences from the WT control: *, $P < 0.05$; **, $P < 0.001$.

in signal transduction and that the phenotypes caused by overexpression of *pe19* are due to the function of PE19 itself.

Overexpression of *pe19* does not cause sensitivity to acid or nitrosative stress. We previously demonstrated that Δ*pstA1* bacteria are more sensitive to nitrosative stress, and this stress sensitivity can be reversed by deletion of *regX3* (33). These data suggested that a RegX3-dependent factor causes sensitivity to reactive nitrogen species. To test whether sensitivity to nitrosative stress also might be caused by overexpression of *pe19*, we analyzed the Δ*pe19* deletion mutants for resistance to the nitric oxide donor DETA-NO. The Δ*pe19* deletion did not cause any significant change in sensitivity to DETA-NO (Fig. 6A). These data suggest that sensitivity to nitrosative stress is caused by a RegX3-dependent factor other than PE19.

In preliminary experiments, we tested sensitivity to nitrosative stress using an acidified nitrate medium (46). Control experiments revealed that Δ*pstA1* bacteria are hypersensitive to mild acid, pH 5.5 (Fig. 6B). Survival of the Δ*pstA1* mutant was significantly reduced after 7 days of culture in 7H9, pH 5.5, compared to that of the WT control. Acid sensitivity of the Δ*pstA1* mutant was attributable to aberrant gene expression mediated by RegX3, since the Δ*pstA1* Δ*regX3* mutant was as resistant to acidified 7H9 medium as the WT control (Fig. 6B). Complementation of the *regX3* deletion by the introduction of plasmid-encoded *regX3* restored acid sensitivity (Fig. 6B).

To determine if PE19 is the RegX3-dependent factor responsible for acid sensitivity, we examined sensitivity of the Δ*pe19* mutants to acidified 7H9 medium. The Δ*pe19* mutation did not significantly alter acid resistance in the WT background (Fig. 6C). In contrast, the Δ*pstA1* Δ*pe19* mutant was significantly more sensitive than the Δ*pstA1* parental strain to acidified medium ($P = 0.0138$) (Fig. 6C). These data suggest that a RegX3-regulated factor(s) other than PE19 causes acid sensitivity.

Sensitivity to acid is not mediated by other RegX3-regulated PE or PPE proteins. Since acid sensitivity of the Δ*pstA1* mutant was not attributable to the overexpression of *pe19*, we explored the possibility that the overexpression of other PE and PPE proteins contribute to acid sensitivity. We tested sensitivity of the Δ*pstA1* Δ*ppe25-ppe26* and Δ*pstA1* Δ*pe32-ppe65* mutants to 7H9, pH 5.5. Both of these mutants remained significantly hypersensitive to acidic pH (Fig. 7A and B). Neither of these *pe-ppe* deletions significantly impacted replication in acidified medium in the WT background (Fig. 7A and B). These data suggest that RegX3-regulated factor(s) other than the PE and PPE proteins that we have deleted cause sensitivity of the Δ*pstA1* mutant to mild acid.

Overexpression of *pe19* causes increased cell envelope permeability. Since some PE and PPE proteins are known to localize to the mycobacterial cell wall (3, 7, 8, 34, 36), we predicted that overexpression of *pe19* contributes to stress sensitivity by altering the permeability of the cell envelope. To test this hypothesis, we used an ethidium bromide uptake assay which measures the in-

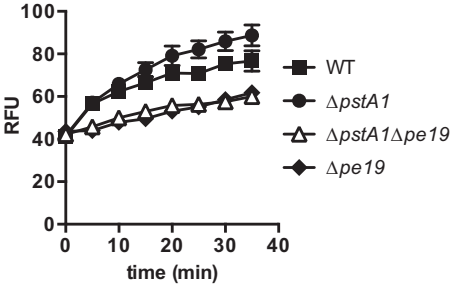

FIG 8 Increased envelope permeability of the Δ*pstA1* mutant is caused by *pe19*. The indicated *M. tuberculosis* strains in the mc^{2}7000 background were incubated with 20 μM ethidium bromide, and uptake rates were determined by measuring emission at 590 nm upon excitation at 530 nm. Data presented are expressed as relative fluorescence units (RFU) and are the means ± standard deviations of triplicate samples from a single experiment. Data are representative of three independent experiments. Uptake rates presented in the text were determined using data between the 5- and 30-min time points and are the means ± standard deviations from three independent experiments.

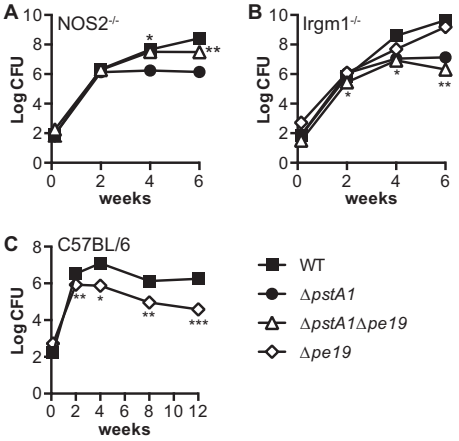

FIG 9 Deletion of *pe19* partially suppresses the replication defect of the Δ*pstA1* mutant in NOS2$^{-/-}$ mice. NOS2$^{-/-}$ (A), Irgm1$^{-/-}$ (B), or C57BL/6J (C) mice were infected by the aerosol route with ~100 CFU of the *M. tuberculosis* WT, Δ*pstA1*, Δ*pstA1* Δ*pe19*, or Δ*pe19* strain. Groups of infected mice ($n = 4$) were euthanized at the indicated time points. Bacterial CFU were enumerated by plating lung homogenates on 7H10 agar and incubating for 3 to 4 weeks at 37°C. Symbols represent means, and error bars indicate standard errors of the means. Results for the Δ*pstA1* Δ*pe19* mutant are from a single experiment and are representative of two independent experiments. All other results are from a single experiment. Asterisks indicate statistically significant differences between Δ*pstA1* and Δ*pstA1* Δ*pe19* mutants (*, $P < 0.05$; **, $P < 0.005$) (A), between both the Δ*pstA1* and Δ*pstA1* Δ*pe19* mutants compared to the WT (*, $P < 0.05$; **, $P < 0.007$) (B), and between Δ*pe19* and WT strains (*, $P < 0.05$; **, $P < 0.005$; ***, $P < 0.001$) (C).

crease in fluorescence of ethidium bromide after uptake and binding to bacterial nucleic acids (43). To facilitate performing these assays, we reconstructed the Δ*pstA1* and Δ*pe19* mutations in the attenuated *M. tuberculosis* strain mc^{2}7000 (H37Rv, ΔRD1, Δ*panCD* [37]). In the mc^{2}7000 background. The Δ*pstA1* mutation caused increased sensitivity to both SDS and H_2O_2, while the Δ*pstA1* Δ*pe19* double mutant was as resistant to these stress conditions as the WT mc^{2}7000 control (see Fig. S1 in the supplemental material). The Δ*pe19* deletion also caused a significant decrease in growth rate of the mc^{2}7000 strain (see Table S4). These data indicate that *pe19* is required for optimal replication and that *pe19* overexpression causes sensitivity to cell wall and oxidative stress in the attenuated mc^{2}7000 background, like in the virulent Erdman strain.

In ethidium bromide uptake assays, we observed a statistically significant 2-fold increase in the uptake rate for the Δ*pstA1* mutant (1.165 ± 0.1225 RFU/min; $P = 0.002$) compared with that of the WT mc^{2}7000 control (0.57 ± 0.0773 RFU/min) (Fig. 8). The Δ*pe19* mutant consistently exhibited a slower initial rate of ethidium bromide uptake, although the steady-state uptake rate (0.523 ± 0.0835 RFU/min) was only modestly slower than that of the WT mc^{2}7000 control (Fig. 8). The Δ*pstA1* Δ*pe19* double mutant exhibited a rate of ethidium bromide uptake (0.489 ± 0.147 RFU/min) similar to that of the WT and Δ*pe19* strains (Fig. 8). These data indicate that overexpression of *pe19* increases permeability of the mycobacterial envelope in the Δ*pstA1* mutant.

To determine if PE19 directly influences cell envelope permeability by localizing to the cell wall, we generated versions of PE19 that were tagged at the C terminus with either the His_6 or HA epitope. It was necessary to construct epitope-tagged PE19 for these experiments due to the high similarly of PE19 to other PE proteins (89.9% identical, 91.9% similar to PE18) that would preclude the specific detection of PE19 with antibodies to either the full-length PE19 or predicted antigenic peptides. C-terminal HA epitope tags previously have been used to determine the localization of the PE domain from other PE proteins (9, 35). The PE19-His_6 and PE19-HA epitope-tagged proteins were functional, since they could complement the H_2O_2 resistance phenotypes of the Δ*pstA1* Δ*pe19* mutant as effectively as untagged PE19 (see Fig. S2 in the supplemental material). However, we were unable to detect either PE19-His_6 or PE19-HA in Western blot experiments performed on the whole-cell lysate and secreted protein fractions from these strains (data not shown).

Overexpression of *pe19* causes attenuation of the Δ*pstA1* mutant in NOS2$^{-/-}$ mice. We previously demonstrated that Δ*pstA1* bacteria are sensitive to host gamma interferon (IFN-γ)-dependent adaptive immune responses. The Δ*pstA1* mutant is attenuated for replication and virulence in mice lacking either the IFN-γ-regulated GTPase Irgm1 or the IFN-γ-inducible nitric oxide synthase NOS2 (33). The attenuation of Δ*pstA1* bacteria in NOS2$^{-/-}$ mice could be partially reversed by deletion of *regX3*, suggesting that the aberrant expression of RegX3-dependent gene(s) causes sensitivity to host immune responses (33). We sought to determine whether the overexpression of *pe19* causes the *in vivo* attenuation of the Δ*pstA1* mutant. Because we previously demonstrated that *M. tuberculosis* can become attenuated due to spontaneous mutations that eliminate the production of the complex cell wall lipid phthiocerol dimycocerosate (PDIM) (38), we first confirmed that the *pe19* deletion did not alter PDIM synthesis (see Fig. S3 in the supplemental material). NOS2$^{-/-}$ mice were infected by the aerosol route with ~100 CFU of the Δ*pstA1* Δ*pe19* mutant, WT Erdman, or the Δ*pstA1* mutant. Deletion of *pe19* partially restored the ability of the Δ*pstA1* mutant to replicate in the lungs of NOS2$^{-/-}$ mice (Fig. 9A). Bacterial loads were significantly higher in the lungs of Δ*pstA1* Δ*pe19*-infected mice than of Δ*pstA1*-infected mice at both 4 weeks ($P = 0.0465$) and 6 weeks ($P = 0.0044$) postinfection (Fig. 9A). Viable CFU recovered from the lungs of Δ*pstA1* Δ*pe19*-infected mice were not significantly different from those of the WT control at any time point. These data suggest that the overexpression of *pe19* sensitizes

the Δ*pstA1* mutant to a host immune response that is independent of nitric oxide production by NOS2.

We previously observed that the deletion of *regX3* did not suppress the replication or virulence defects of the Δ*pstA1* mutant in Irgm1$^{-/-}$ mice (33). However, we were unable to rule out the possibility that a RegX3-regulated factor(s) contributes to these replication and virulence defects, because a Δ*regX3* mutant was similarly attenuated (33). Since the Δ*pe19* deletion partially reversed the replication defect of the Δ*pstA1* mutant in NOS2$^{-/-}$ mice, we tested if *pe19* also was responsible for the attenuation of the Δ*pstA1* mutant in Irgm1$^{-/-}$ mice. We infected Irgm1$^{-/-}$ mice by the aerosol route with ~100 CFU of the Δ*pstA1* Δ*pe19* mutant, WT Erdman, or the Δ*pstA1* mutant. The Δ*pstA1* Δ*pe19* mutant remained significantly attenuated for replication in the lungs of Irgm1$^{-/-}$ mice (Fig. 9B). Viable CFU recovered from the lungs of Irgm1$^{-/-}$ mice infected with the Δ*pstA1* Δ*pe19* mutant were significantly reduced compared to those of the WT control at 2, 4, and 6 weeks postinfection (Fig. 9B). There was no significant difference in CFU recovered from Irgm1$^{-/-}$ mice infected with the Δ*pstA1* or Δ*pstA1* Δ*pe19* mutant at any time point. The Δ*pstA1* Δ*pe19* mutant also was significantly attenuated for virulence in Irgm1$^{-/-}$ mice. While Irgm1$^{-/-}$ mice infected with 100 CFU of WT Erdman succumb rapidly to the infection, with a mean survival time of 38.5 days (33), all 8 mice infected with the Δ*pstA1* Δ*pe19* mutant survived to 16 weeks postinfection, when the experiment was terminated ($P < 0.0001$) (data not shown). To determine if the Δ*pe19* mutation causes attenuation in Irgm1$^{-/-}$ mice, we infected Irgm1$^{-/-}$ mice with the Δ*pe19* mutant. The Δ*pe19* mutant replicated extensively in the lungs of Irgm1$^{-/-}$ mice, with kinetics similar to those of the WT control (Fig. 9B). Bacterial burden in the lungs of Δ*pe19*-infected Irgm1$^{-/-}$ mice was not significantly different from that of the WT control at either the 4- or 6-week time point (Fig. 9B). These data suggest that a factor or factors other than the overexpression of *pe19* cause attenuation of the Δ*pstA1* mutant in Irgm1$^{-/-}$ mice.

Finally, we examined if PE19 is important for the replication or persistence of *M. tuberculosis* in wild-type mice. C57BL/6 mice were infected by the aerosol route with ~100 CFU of WT Erdman or ~500 CFU of the Δ*pe19* mutant. Despite a higher initial inoculum, the Δ*pe19* mutant exhibited a significant replication defect in the lungs over the first 2 weeks of infection (Fig. 9C). After 4 weeks of infection, the number of CFU recovered from the lungs of Δ*pe19*-infected mice began to decline and remained significantly different from that of the WT control (Fig. 9C). The phenotype of the Δ*pe19* mutant in C57BL/6 mice strongly resembled the phenotypes of both the Δ*regX3* and Δ*pstA1* mutants, which also exhibited a persistence defect during the chronic phase of infection (33). These data indicate that PE19 is important for replication and persistence in the lungs of an immunocompetent mammalian host.

DISCUSSION

Although the PE and PPE proteins represent a large fraction of the coding capacity of the *M. tuberculosis* genome, their functions in mycobacterial physiology and virulence remain poorly understood. Since many PE and PPE proteins that have been characterized to date are localized to the cell wall (3, 7, 8, 34–36), we predicted that the aberrant overexpression of these proteins would sensitize *M. tuberculosis* to stress. We demonstrate that the overexpression of the PE protein PE19, which consists of only a 99-amino-acid PE domain, causes sensitivity to specific cell wall and oxidative stress conditions *in vitro* and to NOS2-independent host immune responses *in vivo*. These phenotypes likely are due to a general increase in the permeability of the mycobacterial envelope upon PE19 overexpression that we observed by ethidium bromide uptake assays. We further show that PE19 is necessary for optimal replication both in liquid culture and in the lungs of immunocompetent mice. Together, these data suggest that PE19 has an important and nonredundant role in *M. tuberculosis* physiology and virulence. To our knowledge, this is the first direct association of specific *in vitro* growth, stress sensitivity, and virulence phenotypes with the expression of a single PE protein consisting of only the PE domain in *M. tuberculosis*.

Our previous work demonstrated that an *M. tuberculosis* Δ*pstA1* mutant is sensitive to a variety of stress conditions *in vitro*, including the cell wall-disrupting detergent SDS and the reactive oxygen species H_2O_2, due to constitutive activation of the RegX3 DNA-binding response regulator (33). These data suggested that the constitutive expression of a RegX3-regulated factor or factors causes sensitivity to stress. Because the pleiotropic stress sensitivity of the Δ*pstA1* mutant was reminiscent of *M. tuberculosis* strains with cell wall defects (47), we targeted the RegX3-regulated PE and PPE proteins for our analysis. By deleting potential *pe-ppe* gene pairs or operons and ultimately making single gene deletions, we demonstrate that the overexpression of a single *pe* gene, *pe19*, is responsible for the sensitivity of the Δ*pstA1* mutant to both SDS and H_2O_2. The overexpression of *pe19* also is sufficient to cause sensitivity to these two stress conditions in WT *M. tuberculosis*. It is likely that the increased sensitivity to stress caused by *pe19* overexpression is due to an increase in the permeability of the mycobacterial envelope, which we observed using ethidium bromide uptake assays. Although the detergent SDS and the reactive oxygen species H_2O_2 are quite different stressors that are predicted to have different effects on the cell, it is possible that the general increased permeability of the *M. tuberculosis* envelope in the Δ*pstA1* mutant allows increased penetration of these compounds. Indeed, *M. tuberculosis* mutant strains with predicted defects in cell wall biogenesis were similarly sensitive to both SDS and H_2O_2 *in vitro* (47), suggesting that alterations to the cell wall can influence the ability to resist both of these stressors.

The overexpression of *pe19* also contributes to the sensitivity of the Δ*pstA1* mutant to host immune responses *in vivo*, since the deletion of *pe19* partially restored the ability to replicate in the lungs of NOS2$^{-/-}$ mice. This suggests that the overexpression of PE19 causes sensitivity to an immune response other than nitric oxide produced by NOS2. It is possible that the increased expression of PE19 sensitizes Δ*pstA1* mutant bacteria to reactive oxygen species produced by the phagocyte oxidase (phox), since the overexpression of *pe19* caused sensitivity to H_2O_2 *in vitro*. However, *pe19* is not the only factor that contributes to the attenuation of the Δ*pstA1* mutant, since the Δ*pstA1* Δ*pe19* double mutant is severely attenuated for replication in the lungs and virulence in Irgm1$^{-/-}$ mice. The Δ*pstA1* Δ*pe19* bacteria might remain sensitive to either phagosome acidification or nitric oxide produced by NOS2 in Irgm1$^{-/-}$ mice, since the Δ*pstA1* Δ*pe19* mutant remained hypersensitive to both acid and nitrosative stress *in vitro*. Together, our data indicate that the Δ*pstA1* mutant is attenuated due to pleiotropic changes in gene expression caused by the constitutive activation of RegX3, of which PE19 overexpression is only one part. The aberrant expression of other RegX3-regulated

factors likely contributes to sensitivity to acid, nitrosative stress, and host immunity.

In addition to causing a general alteration in the permeability of the *M. tuberculosis* envelope, PE19 also is necessary for optimal replication both *in vitro* and *in vivo* in the lungs of wild-type mice. PE19 may enhance the permeability of the envelope to specific nutrients that are necessary for *M. tuberculosis* replication *in vitro* and *in vivo*. However, the Δ*pe19* mutants had a relatively modest decrease in growth rate compared with that of either the Δ*ppe27-pe19* or Δ*ppe25-pe19* mutant. We were not able to fully complement the growth defect of the Δ*ppe27-pe19* mutant by providing the *ppe27-pe19* locus *in trans*, suggesting the polarity of this deletion on the expression of other genes. A large 426-bp intergenic region between *ppe27* and *pe19* that contains multiple transcription start sites (48) also is deleted in the Δ*ppe27-pe19* mutant. We have evidence that this intergenic region contains a RegX3-dependent promoter that drives the expression of genes 3′ to *pe19*, which include conserved components and secreted substrates of the specialized type VII protein secretion system ESX-5 (S. R. Elliott and A. D. Tischler, unpublished data). We speculate that the more substantial growth defect of the Δ*ppe25-pe19* and Δ*ppe27-pe19* mutants is due to the decreased production of ESX-5 core components, which are essential for growth *in vitro* (49, 50).

Our data suggest that PE19 has a nonredundant function in *M. tuberculosis* physiology. This is surprising, since PE19 has high similarity to the PE18 protein that also is encoded by the *ppe25-pe19* locus (89.9% identical, 91.9% similar). However, the deletion of *pe18* (in the Δ*ppe25-ppe26* mutant) did not influence either the growth rate of *M. tuberculosis* or the sensitivity of the Δ*pstA1* mutant to stress. PE proteins are thought to form heterodimeric complexes with a partner PPE protein based on the crystal structure of the PE/PPE pair PE25 and PPE41 (51). It is possible that the sequence differences between PE19 and PE18 enable these proteins to form heterodimers with different PPE partner proteins that have different functions. However, it is unclear which PPE proteins might interact with PE19 to mediate its functions. Many *pe* genes are located adjacent to and coexpressed with a *ppe* gene (2, 52, 53). These co-operonic *pe* and *ppe* genes are assumed to form heterodimeric complexes like PE25/PPE41. However, we were unable to recapitulate the phenotypes associated with the deletion of *pe19* by deleting the *ppe* genes located in the *ppe25-pe19* locus. It is possible that PE19 can interact with several different PPE proteins to carry out its function. In this scenario, it would be necessary to delete all of the *ppe* genes that encode PE19 partners to observe changes in growth rate or stress sensitivity similar to those caused by the deletion of *pe19*.

The reduced growth rate of Δ*pe19* mutant bacteria and association of PE19 overexpression with sensitivity to cell wall stress and increased cell envelope permeability suggest that PE19 is localized to the cell wall and, along with its potential PPE partner(s), influences cell wall architecture or permeability. A recent structural study of EspB, an *M. tuberculosis* protein secreted by the ESX-1 type VII secretion system, revealed that this protein adopts a conformation similar to that of the PE25/PPE41 structure and forms ring-shaped multimers (54). PE19 and its PPE partner(s) may form similar multimers that localize to the cell wall and influence its permeability. Since *pe19* expression is regulated by the P_i starvation-responsive Pst/SenX3-RegX3 signal transduction system, we speculate that PE19 is specifically involved in permeabilizing the cell wall to allow the uptake of nutrients that contain P_i. We attempted to determine the localization of PE19 by expressing C-terminal epitope-tagged versions of the protein. Although these epitope-tagged PE19 proteins apparently were functional, since they could complement stress sensitivity phenotypes associated with the Δ*pe19* mutation, we were unable to detect PE19 in Western blots. It is possible that PE19 is produced at a low level or is unstable, such that the protein is not present in sufficient quantities for detection by Western blotting. Alternatively, PE19 may be proteolytically processed at the C terminus, which would remove the C-terminal epitope tags we engineered. It may be necessary to use more sensitive or larger epitope tags (e.g., green fluorescent protein) or to N-terminally tag PE19 to determine its localization. Our future work will focus on further biochemical characterization of PE19 to determine its localization, interacting partners, and potential functions in nutrient acquisition.

ACKNOWLEDGMENTS

We thank Manisha Lotlikar and Laetitia Martin for expert technical assistance with animal experiments, John Hartzheim for constructing pMV*pe19*, Greg Taylor for providing Irgm1$^{-/-}$ mice, and Bill Jacobs for providing the mc^{2}7000 strain.

This work was supported by an Irvington Postdoctoral Fellowship of the Cancer Research Institute (A.D.T.), Swiss National Science Foundation grant 310030_156945 (J.D.M.), and institutional start-up funds from the University of Minnesota (A.D.T.).

FUNDING INFORMATION

University of Minnesota (UM) provided funding to Anna D. Tischler. Schweizerischer Nationalfonds zur Förderung der Wissenschaftlichen Forschung (SNF) provided funding to John D. McKinney under grant number 310030_156945. Cancer Research Institute (CRI) provided funding to Anna D. Tischler.

The funders had no role in study design, data collection and interpretation, or the decision to submit the work for publication.

REFERENCES

1. **Cole ST, Brosch R, Parkhill J, Garnier T, Churcher C, Harris D, Gordon SV, Eiglmeier K, Gas S, Barry CEI, Takala F, Badcock K, Basham D, Brown D, Chillingworth T, Connor R, Davies R, Devlin K, Feltwell T, Gentles S, Hamlin N, Holroyd S, Hornsby T, Jagels K, Krogh A, McLean J, Moule S, Murphy L, Oliver K, Osborne J, Quail MA, Rajandream MA, Rogers J, Rutter S, Seeger K, Skelton J, Squares R, Squares S, Sulston JE, Taylor K, Whitehead S, Barrell BG.** 1998. Deciphering the biology of *Mycobacterium tuberculosis* from the complete genome sequence. Nature **393:**537–544. http://dx.doi.org/10.1038/31159.
2. **Gey van Pittius NC, Sampson SL, Lee H, Kim Y, van Helden PD, Warren RM.** 2006. Evolution and expansion of the *Mycobacterium tuberculosis* PE and PPE multigene families and their association with the duplication of the ESAT-6 (*esx*) gene cluster regions. BMC Evol Biol **6:**95. http://dx.doi.org/10.1186/1471-2148-6-95.
3. **Delogu G, Pusceddu C, Bua A, Fadda G, Brennan MJ, Zanetti S.** 2004. Rv1818c-encoded PE_PGRS protein of *Mycobacterium tuberculosis* is surface exposed and influences bacterial cell structure. Mol Microbiol **52:** 725–733. http://dx.doi.org/10.1111/j.1365-2958.2004.04007.x.
4. **Abdallah AM, Verboom T, Hannes F, Safi M, Strong M, Eisenberg D, Musters RJ, Vandenbrouck-Grauls CM, Appelmelk BJ, Luirink J, Bitter W.** 2006. A specific secretion system mediates PPE41 transport in pathogenic mycobacteria. Mol Microbiol **62:**667–679. http://dx.doi.org/10.1111/j.1365-2958.2006.05409.x.
5. **Abdallah AM, Verboom T, Weerdenburg EM, Gey van Pittius NC, Mahasha PW, Jimenez C, Parra M, Cadieux N, Brennan MJ, Appelmelk BJ, Bitter W.** 2009. PPE and PE_PGRS proteins of *Mycobacterium marinum* are transported via the type VII secretion system ESX-5. Mol Microbiol **73:**329–340. http://dx.doi.org/10.1111/j.1365-2958.2009.06783.x.
6. **Bottai D, Di Luca M, Majlessi L, Frigui W, Simeone R, Sayes F, Bitter W, Brennan MJ, Leclerc C, Batoni G, Campa M, Brosch R, Esin S.** 2012.

Disruption of the ESX-5 system of *Mycobacterium tuberculosis* causes loss of PPE protein secretion, reduction of cell wall integrity and strong attenuation. Mol Microbiol **83:**1195–1209. http://dx.doi.org/10.1111/j.1365-2958.2012.08001.x.

7. **Cascioferro A, Daleke MH, Ventura M, Dona V, Delogu G, Palú G, Bitter W, Manganelli R.** 2011. Functional dissection of the PE domain responsible for translocation of PE_PGRS33 across the mycobacterial cell wall. PLoS One **6:**e27713. http://dx.doi.org/10.1371/journal.pone.0027713.
8. **Daleke MH, Cascioferro A, de Punder K, Ummels R, Abdallah AM, van der Wel N, Peters PJ, Luirink J, Manganelli R, Bitter W.** 2011. Conserved Pro-Glu (PE) and Pro-Pro-Glu (PPE) protein domains target LipY lipases of pathogenic mycobacteria to the cell surface via the ESX-5 pathway. J Biol Chem **286:**19024–19034. http://dx.doi.org/10.1074/jbc.M110.204966.
9. **Daleke MH, Ummels R, Bawono P, Heringa J, Vandenbrouck-Grauls CM, Luirink J, Bitter W.** 2012. General secretion signal for the mycobacterial type VII secretion pathway. Proc Natl Acad Sci U S A **109:**11342–11347. http://dx.doi.org/10.1073/pnas.1119453109.
10. **Talarico S, Cave MD, Marrs CF, Foxman B, Zhang L, Yang Z.** 2005. Variation of the *Mycobacterium tuberculosis* PE_PGRS33 gene among clinical isolates. J Clin Microbiol **43:**4954–4960. http://dx.doi.org/10.1128/JCM.43.10.4954-4960.2005.
11. **Talarico S, Zhang L, Marrs CF, Foxman B, Cave MD, Brennan MJ, Yang Z.** 2008. *Mycobacterium tuberculosis* PE_PGRS16 and PE_PGRS26 genetic polymorphism among clinical isolates. Tuberculosis (Edinb) **88:**283–294. http://dx.doi.org/10.1016/j.tube.2008.01.001.
12. **Karboul A, Mazza A, Gey van Pittius NC, Ho JL, Brousseau R, Mardassi H.** 2008. Frequent homologous recombination events in *Mycobacterium tuberculosis* PE/PPE multigene families: potential role in antigenic variability. J Bacteriol **190:**7838–7846. http://dx.doi.org/10.1128/JB.00827-08.
13. **Ford CB, Lin PL, Chase MR, Shah RR, Iartchouk O, Galagan J, Mohaideen N, Ioerger TR, Sacchettini JC, Lipsitch M, Flynn JL, Fortune SM.** 2011. Use of whole genome sequencing to estimate the mutation rate of *Mycobacterium tuberculosis* during latent infection. Nat Genet **43:**482–486. http://dx.doi.org/10.1038/ng.811.
14. **McEvoy CRE, Cloete R, Müller B, Schürch AC, van Helden PD, Gagneux S, Warren RM, Gey van Pittius NC.** 2012. Comparative analysis of *Mycobacterium tuberculosis pe* and *ppe* genes reveals high sequence variation and an apparent absence of selective constraints. PLoS One **7:**e30593. http://dx.doi.org/10.1371/journal.pone.0030593.
15. **Vordermeier HM, Hewinson RG, Wilkinson RJ, Wilkinson KA, Gideon HP, Young DB, Sampson SL.** 2012. Conserved immune recognition hierarchy of mycobacterial PE/PPE proteins during infection in natural hosts. PLoS One **7:**e40890. http://dx.doi.org/10.1371/journal.pone.0040890.
16. **Sayes F, Sun L, Di Luca M, Simeone R, Degaiffier N, Fiette L, Esin S, Brosch R, Bottai D, Leclerc C, Majlessi L.** 2012. Strong immunogenicity and cross-reactivity of *Mycobacterium tuberculosis* ESX-5 type VII secretion-encoded PE-PPE proteins predicts vaccine potential. Cell Host Microbe **11:**352–363. http://dx.doi.org/10.1016/j.chom.2012.03.003.
17. **Arlehamn CSL, Gerasimova A, Mele F, Henderson R, Swann J, Greenbaum JA, Kim Y, Sidney J, James EA, Taplitz R, McKinney DM, Kwok WW, Grey H, Sallusto F, Peters B, Sette A.** 2013. Memory T cells in latent *Mycobacterium tuberculosis* infection are directed against three antigenic islands and are largely contained in a $CXCR3^+CCR6^+$ Th1 subset. PLoS Pathog **9:**e1003130. http://dx.doi.org/10.1371/journal.ppat.1003130.
18. **Sassetti CM, Boyd DH, Rubin EJ.** 2003. Genes required for mycobacterial growth defined by high density mutagenesis. Mol Microbiol **48:**77–84. http://dx.doi.org/10.1046/j.1365-2958.2003.03425.x.
19. **Sassetti CM, Rubin EJ.** 2003. Genetic requirements for mycobacterial survival during infection. Proc Natl Acad Sci U S A **100:**12989–12994. http://dx.doi.org/10.1073/pnas.2134250100.
20. **Griffin JE, Gawronski JD, Dejesus MA, Ioerger TR, Akerley BJ, Sassetti CM.** 2011. High-resolution phenotypic profiling defines genes essential for mycobacterial growth and cholesterol catabolism. PLoS Pathog **7:**e1002251. http://dx.doi.org/10.1371/journal.ppat.1002251.
21. **Iantomasi R, Sali M, Cascioferro A, Palucci I, Zumbo A, Soldini S, Rocca S, Greco E, Maulucci G, De Spirito M, Fraziano M, Fadda G, Manganelli R, Delogu G.** 2012. PE_PGRS30 is required for full virulence of *Mycobacterium tuberculosis*. Cell Microbiol **14:**356–367. http://dx.doi.org/10.1111/j.1462-5822.2011.01721.x.
22. **Stewart GR, Patel J, Robertson BD, Rae A, Young DB.** 2005. Mycobacterial mutants with defective control of phagosomal acidification. PLoS Pathog **1:**269–278.
23. **Brodin P, Poquet Y, Levillain F, Peguillet I, Lorrouy-Maumus G, Gilleron M, Ewann F, Christophe T, Jang J, Jang MS, Park SJ, Rauzier J, Carralot J-P, Shrimpton R, Genovesio A, Gonzalo-Asenio JA, Puzo G, Martin C, Brosch R, Stewart GR, Gicquel B, Neyrolles O.** 2010. High content phenotypic cell-based visual screen identifies *Mycobacterium tuberculosis* acyltrehalose-containing glycolipids involved in phagosome remodeling. PLoS Pathog **9:**e1001100.
24. **Deb C, Daniel J, Sirakova TD, Abomoelak B, Dubey VS, Kolattukudy PE.** 2006. A novel lipase belonging to the hormone-sensitive lipase family induced under starvation to utilize stored triacylglycerol in *Mycobacterium tuberculosis*. J Biol Chem **281:**3866–3875. http://dx.doi.org/10.1074/jbc.M505556200.
25. **Mishra KC, de Chastellier C, Narayana Y, Bifani P, Brown AK, Besra GS, Katoch VM, Joshi B, Balaji KN, Kremer L.** 2008. Functional role of the PE domain and immunogenicity of the *Mycobacterium tuberculosis* triacylglycerol hydrolase LipY. Infect Immun **76:**127–140. http://dx.doi.org/10.1128/IAI.00410-07.
26. **Chaturvedi R, Bansal K, Narayana Y, Kapoor N, Sukumar N, Togarsimalemath SK, Chandra N, Mishra S, Ajitkumar P, Joshi B, Katoch VM, Patil SA, Balaji KN.** 2010. The multifunctional PE_PGRS11 protein from *Mycobacterium tuberculosis* plays a role in regulating resistance to oxidative stress. J Biol Chem **285:**30389–30403. http://dx.doi.org/10.1074/jbc.M110.135251.
27. **Sultana R, Tanneeru K, Guruprasad L.** 2011. The PE-PPE domain in Mycobacterium reveals a serine α/β hydrolase fold and function: an *in-silico* analysis. PLoS One **6:**e16745. http://dx.doi.org/10.1371/journal.pone.0016745.
28. **Sultana R, Vemula MH, Banerjee S, Guruprasad L.** 2013. The PE16 (Rv1430) of *Mycobacterium tuberculosis* is an esterase belonging to serine hydrolase superfamily of proteins. PLoS One **8:**e55320. http://dx.doi.org/10.1371/journal.pone.0055320.
29. **Voskuil MI, Schnappinger D, Rutherford R, Liu Y, Schoolnik GK.** 2004. Regulation of the *Mycobacterium tuberculosis* PE/PPE genes. Tuberculosis (Edinb) **84:**256–262. http://dx.doi.org/10.1016/j.tube.2003.12.014.
30. **Sampson SL.** 2011. Mycobacterial PE/PPE proteins at the host-pathogen interface. Clin Dev Immunol **2011:**497203.
31. **Fishbein S, van Wyk N, Warren RM, Sampson SL.** 2015. Phylogeny to function: PE/PPE protein evolution and impact on *Mycobacterium tuberculosis* pathogenicity. Mol Microbiol **96:**901–916. http://dx.doi.org/10.1111/mmi.12981.
32. **Ramakrishnan L, Federspiel NA, Falkow S.** 2000. Granuloma-specific expression of Mycobacterium virulence proteins from the glycine-rich PE-PGRS family. Science **288:**1436–1439. http://dx.doi.org/10.1126/science.288.5470.1436.
33. **Tischler AD, Leistikow RL, Kirksey MA, Voskuil MI, McKinney JD.** 2013. *Mycobacterium tuberculosis* requires phosphate-responsive gene regulation to resist host immunity. Infect Immun **81:**317–328. http://dx.doi.org/10.1128/IAI.01136-12.
34. **Sampson SL, Lukey P, Warren RM, van Helden PD, Richardson M, Everett MJ.** 2001. Expression, characterization and subcellular localization of the *Mycobacterium tuberculosis* PPE gene Rv1917c. Tuberculosis (Edinb) **81:**305–317. http://dx.doi.org/10.1054/tube.2001.0304.
35. **Cascioferro A, Delogu G, Colone M, Sali M, Stringaro A, Arancia G, Fadda G, Palu G, Manganelli R.** 2007. PE is a functional domain responsible for protein translocation and localization on mycobacterial cell wall. Mol Microbiol **66:**1536–1547.
36. **Dona V, Ventura M, Sali M, Cascioferro A, Provvedi R, Palu G, Delogu G, Manganelli R.** 2013. The PPE domain of PPE17 is responsible for its surface localization and can be used to express heterologous proteins on the mycobacterial surface. PLoS One **8:**e57517. http://dx.doi.org/10.1371/journal.pone.0057517.
37. **Sambandamurthy VK, Derrick SC, Hsu T, Chen B, Larsen MH, Jalapathy KV, Chen M, Kim J, Porcelli SA, Chan J, Morris SL, Jacobs WR, Jr.** 2006. *Mycobacterium tuberculosis* Δ*RD1* Δ*panCD*: a safe and limited replicating mutant strain that protects immunocompetent and immunocompromised mice against experimental tuberculosis. Vaccine **24:**6309–6320. http://dx.doi.org/10.1016/j.vaccine.2006.05.097.
38. **Kirksey MA, Tischler AD, Siméone R, Hisert KB, Uplekar S, Guilhot C, McKinney JD.** 2011. Spontaneous phthiocerol dimycocerosate-deficient variants of *Mycobacterium tuberculosis* are susceptible to gamma interfer-

on-mediated immunity. Infect Immun **79:**2829–2838. http://dx.doi.org/10.1128/IAI.00097-11.
39. **Pavelka MS, Jr, Jacobs WR, Jr.** 1999. Comparison of the construction of unmarked deletion mutations in *Mycobacterium smegmatis*, *Mycobacterium bovis* Bacillus Calmette-Guerin, and *Mycobacterium tuberculosis* H37Rv by allelic exchange. J Bacteriol **181:**4780–4789.
40. **Parish T, Stoker NG.** 2000. Use of a flexible cassette method to generate a double unmarked *Mycobacterium tuberculosis tlyA plcABC* mutant by gene replacement. Microbiology **146:**1969–1975. http://dx.doi.org/10.1099/00221287-146-8-1969.
41. **Larsen MH, Biermann K, Tandberg S, Hsu T, Jacobs WR, Jr.** 2007. Genetic manipulation of *Mycobacterium tuberculosis*. Curr Protoc Microbiol Chapter **10:**Unit 10A.2.
42. **Vandal OH, Nathan CF, Ehrt S.** 2009. Acid resistance in *Mycobacterium tuberculosis*. J Bacteriol **191:**4714–4721. http://dx.doi.org/10.1128/JB.00305-09.
43. **Danilchanka O, Mailaender C, Niederweis M.** 2008. Identification of a novel multidrug efflux pump of *Mycobacterium tuberculosis*. Antimicrob Agents Chemother **52:**2503–2511. http://dx.doi.org/10.1128/AAC.00298-08.
44. **Collazo CM, Yap GS, Sempowski GD, Lusby KC, Tessarollo L, Vande Woude GF, Sher A, Taylor GA.** 2001. Inactivation of LRG-47 and IRG-47 reveals a family of interferon γ-inducible genes with essential, pathogen-specific roles in resistance to infection. J Exp Med **194:**181–187. http://dx.doi.org/10.1084/jem.194.2.181.
45. **National Research Council.** 2011. Guide for the care and use of laboratory animals, 8th ed. National Academies Press, Washington, DC.
46. **Darwin KH, Ehrt S, Gutierrez-Ramos J-C, Weich N, Nathan CF.** 2003. The proteasome of *Mycobacterium tuberculosis* is required for resistance to nitric oxide. Science **302:**1963–1966. http://dx.doi.org/10.1126/science.1091176.
47. **Vandal OH, Roberts JA, Odaira T, Schnappinger D, Nathan CF, Ehrt S.** 2009. Acid-susceptible mutants of *Mycobacterium tuberculosis* share hypersusceptibility to cell wall and oxidative stress and to the host environment. J Bacteriol **191:**625–631. http://dx.doi.org/10.1128/JB.00932-08.
48. **Shell SS, Wang J, Lapierre P, Mir M, Chase MR, Pyle MM, Gawande R, Ahmad R, Sarracino DA, Ioerger TR, Fortune SM, Derbyshire KM, Wade JT, Gray TA.** 2015. Leaderless transcripts and small proteins are common features of the mycobacterial translational landscape. PLoS Genet **4:**e1005641.
49. **Di Luca M, Bottai D, Batoni G, Orgeur M, Aulicino A, Counoupas C, Campa M, Brosch R, Esin S.** 2012. The ESX-5 associated *eccB5-eccC5* locus is essential for *Mycobacterium tuberculosis* viability. PLoS One **7:**e52059. http://dx.doi.org/10.1371/journal.pone.0052059.
50. **Ates LS, Ummels R, Commandeur S, van der Weerd R, Sparrius M, Weerdenburg E, Alber M, Kalscheuer R, Piersma SR, Abdallah AM, El Ghany MA, Abdel-Haleem AM, Pain A, Jiménez CR, Bitter W, Houben ENG.** 2015. Essential role of the ESX-5 secretion system in outer membrane permeability of pathogenic mycobacteria. PLoS Genet **11:**e1005190. http://dx.doi.org/10.1371/journal.pgen.1005190.
51. **Strong M, Sawaya MR, Wang S, Phillips M, Cascio D, Eisenberg D.** 2006. Toward the structural genomics of complexes: crystal structure of a PE/PPE protein complex from *Mycobacterium tuberculosis*. Proc Natl Acad Sci U S A **103:**8060–8065. http://dx.doi.org/10.1073/pnas.0602606103.
52. **Tundup S, Akhter Y, Thiagarajan D, Hasnain SE.** 2006. Clusters of PE and PPE genes of *Mycobacterium tuberculosis* are organized in operons: evidence that PE Rv2431c is co-transcribed with PPE Rv2430c and their gene products interact with each other. FEBS Lett **580:**1285–1293. http://dx.doi.org/10.1016/j.febslet.2006.01.042.
53. **Tiwari BM, Kannan N, Vemu L, Raghunand TR.** 2012. The *Mycobacterium tuberculosis* PE proteins Rv0285 and Rv1386 modulate innate immunity and mediate bacillary survival in macrophages. PLoS One **7:**e51686. http://dx.doi.org/10.1371/journal.pone.0051686.
54. **Solomonson M, Setiaputra D, Makepeace KAT, Lameignere E, Petrotchenko EV, Conrady DG, Bergeron JR, Vuckovic M, DiMaio F, Borchers CH, Yip CK, Strynadka NCJ.** 2015. Structure of EspB from the ESX-1 Type VII secretion system and insights into its export mechanism. Structure **23:**571–583. http://dx.doi.org/10.1016/j.str.2015.01.002.